ORIGINAL PAPER

RJME
Romanian Journal of Morphology & Embryology
http://www.rjme.ro/

Microglial morphology determined with confocal and two-photon laser scanning microscopy

SMARANDA IOANA MITRAN[1)], EMILIA BURADA[1)], CORNELIA-ANDREEA TĂNASIE[1)], NICOLAE CĂTĂLIN MANEA[2)], MIHAI CĂLIN CIORBAGIU[3)], CECIL SORIN MIREA[3)], TUDOR-ADRIAN BĂLŞEANU[1,4)]

[1)]*Department of Functional Sciences, University of Medicine and Pharmacy of Craiova, Romania*

[2)]*Department of Informatics, Communication and Statistics, University of Medicine and Pharmacy of Craiova, Romania*

[3)]*Department of Surgery, University of Medicine and Pharmacy of Craiova, Romania*

[4)]*Experimental Research Center for Normal and Pathological Aging, University of Medicine and Pharmacy of Craiova, Romania*

Abstract

Microglia are the first and main form of active immune defense in the nervous system. The immune status of microglia is directly correlated to their morphology. Therefore, microglia morphology is used to distinguish between active and surveilling microglia. For the actual paper, we used confocal laser scanning microscopy (cLSM) and two-photon laser scanning microscopy (2P-LSM), to investigate microglia morphology of 14–16 weeks old male, transgenic mice (n=6). After obtaining, *in vivo* and fixed tissue, single cells images, we manually tracked individually branch segments of normal microglia. The total number of branches and their overall length were analyzed. Additionally, the number and mean length of each branch order were measured. The overall microglia branching morphology was not different between the two acquisition methods. However, a higher number of fifth branches was observed using cLSM and 2P-LSM, in both fixed and *in vivo* tissue. Although results from the two methods are mainly comparable, small differences between them should be taken in consideration when formulating an activating/surveilling conclusion that is purely based on pure microscopic findings. Furthermore, in our opinion, due to their highly dynamic nature, microglia should be carefully labeled as resting or active, taking also into consideration the imaging method used to obtain the data.

Keywords: microglia morphology, confocal microscopy, two-photon laser scanning microscopy.

Introduction

Microglia are resident immune cells of the central nervous system (CNS) with key roles in neuroinflammation due to their production of proinflammatory cytokines and free radicals [1]. Microglia activation is considered to be a morphological marker of this neuroinflammation [2–4] due to specific microglia morphology change directly linked to pathology [4–6]. As such, specific microglia morphology changes are seen as a sign of abnormality within the CNS. However, a specific microglia marker, able to identify the immune status of these cells, has not been identified and a clear-cut point in the immune activation of microglia has yet to be established. As conformational changes have been observed, many researchers tried to characterize them [7–9]. This attempts have been made using different microscopy techniques like wide field [10, 11] or fluorescence microscopy [12], and different approaches from fixed tissue [10–12], whilst others used *in vivo* models [6, 8]. Other laser-based imaging methods have been used to study cellular dynamics in the brain, such as optical coherence tomography (OCT) [13, 14] but have so far been ineffective on a cellular level.

One of the main problems in studying microglia morphology is that most studies have been focused on changes within neuroinflammation diseases [15–18] or in aging [19, 20], while very few have quantified, in detail, microglia arborization in the normal adult brain [21, 22]. Several reports have discussed microglial responses to changes both in the environment and stress by active branch remodeling [22, 23], thus demonstrating that the relationship between microglia morphology and function is more complex than was initially thought. This limited underestimation could be due to the static way in which a highly dynamic cell like microglia was studied [10, 11]. However, as it is one of the most dynamic cells in the human body, quantifying microglia morphology can be difficult and one should take into consideration other factors such as perfusion techniques that have been showed to have a significant impact on microglia morphology [24, 25].

In light of this observation, we decided to investigate how modern techniques like confocal laser scanning microscopy (cLSM) and two-photon laser scanning microscopy (2P-LSM) perceive microglia morphology in a normal mouse brain. Both laser scanning methods are highly effective tools to investigate morphological changes that can appear in the normal brain and as such these technologies have been used in a lot of neuroscience studies. Their superior spatial resolution compared with other optical imaging acquisition systems makes them ideal for structural detailing of cell morphology [26]. Although, both have a similar working principle, it should be noted that a clear difference in image quality exists between cLSM and 2P-LSM, due to a small loss in spatial resolution when using 2P-LSM [27]. This can be mostly explained by the different sample used to investigate tissue. The main advantage of 2P-LSM is the possibility of singular or chronicle *in vivo* imaging, which allows the observation of cell behavior over a long-time span.

There are many papers focusing on the technical differences between cLSM and 2P-LSM [28, 29]. However, data generated in structural studies reveals different aspects of microglia morphological changes in the injured tissue [7]. This can be a direct consequence on the method used to generate the structural overview of microglia. The purpose of this paper is not to focus on the technical differences of the two methods, but rather investigate the difference of microglia morphology obtained by cLSM and 2P-LSM.

Materials and Methods

Animal preparation for *in vivo* imaging

Transgenic CXCR mice, that have an enhanced green fluorescent protein (EGFP) fused to a transmembrane CX3C chemokine receptor {TgH(CX3CR1-EGFP) [30]} (n=6) (14–16 weeks old males), were anesthetized with an intraperitoneal injection of Ketamine [120 mg/kg body weight (b.w.)]/Xylazine (12 mg/kg b.w.).

The temperature was maintained at 36–37°C, placing the animal, during the imaging sessions, on a heating blanket, while monitoring was made by a rectal probe. During anesthesia, mice were closely observed: pinch withdrawal, eyelid reflex, corneal reflex, vibrissae movements and respiration rate. The cranial window for the experiment was implanted over the right somato-sensory cortex (between -0.5 to -1 mm post bregma and 1.0 to 3.5 mm lateral) [31]. To maintain it stable a custom-made metal holder was attached to the skull using dental acrylic cement. During craniotomy, while drilling, saline solution was periodically added to the skull not to damage the underlying cortex by induced heat. For the same reason, drilling was interrupted from time to time to permit heat dissipation. To eliminate the possible side effects of surgery only cells deeper than 50 µm below the pial surface were image analyzed, as they showed no changes in motility or morphology.

Perfusion and fixation

After the initial perfusion with 1× phosphate-buffered saline (PBS), 4% paraformaldehyde (PFA) was pumped in the animal's circulatory system allowing a slow whole-body fixation. The brain was removed and post-fixed overnight in 4% PFA. The fixed brain was used for vibratome slicing using a Leica VT1000S vibratome and mounted in Aqua poly mount (Polysciences).

Two-photon laser scanning microscopy

In vivo and fixed two-photon imaging was performed using a custom-built two-photon laser-scanning microscope. All acquired images were taken using a 20× water-immersion objective lens (0.8 NA; Carl Zeiss, Jena). Scanning and imaging were controlled by a custom-written software [32]. The excitation laser intensity was kept at a minimum to minimize photo damage but was high enough to obtain a good signal-to-noise ratio. Image acquisition was made with the laser (Chameleon Ultra II, Ti:Sapphire Laser, Coherent) set to 910 nm. Emission was detected using a photomultiplier tube (R6357, Hamamatsu). Both *in vivo* and *in vitro* image acquisition was made without averaging at a pixel time of 5.7 µs, as to keep 2P-LSM characteristics used for *in vivo* studies, as 2P-LSM is not normally used to image slices. Image stacks of small, cortical volumes (15–30 focal planes with 1–2 µm axial spacing) were generated for data analysis [33].

Confocal laser scanning microscopy

cLSM stacks were obtained using a LSM 710 (Carl Zeiss, Jena) with a 40×/1 objective (Plan-Aprochomat; 4 Oil DIC (UV) VIS-IR M 27). Appropriate excitation/emission filters were used to detect the EGFP bound to microglia membrane. The excitation was made using a Lasos Argon laser (454 nm to 514 nm). The fluorescence protein was excited at 488 nm and a z-stack was made imaging at 1 µm intervals. All data was then processed using Zen (Zeiss) and ImageJ software. The pixel time of all confocal images was 6.2 µs, with a 12-time averaging. The resulting images were 212.55×212.55 µm (512×512 pixel).

Data analysis

To analyze microglia morphology, a semi-manual method was used [34]. Cells that were analyzed were manually selected from the acquired stacks. This was done in such way that each image would display as much of the microglia branching tree as possible. A total number of 23 cells (cLSM) and 25 cells (2P-LSM) were taken into consideration for analysis. After branch isolation and their order assignment (Figure 1), the total branch number, the total length, the number and mean length of each branch order were analyzed using GraphPad Prism 6 and Microsoft Excel. Two-way analysis of variance (ANOVA) and Student's t-test were used to evaluate statistical difference. All figures show mean value and standard error of the mean the statistical significance is displayed as follows: * – p<0.05, ** – p<0.01 and *** – p<0.001.

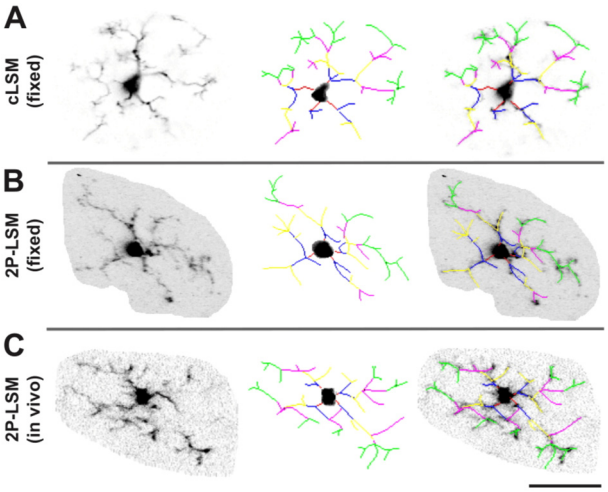

Figure 1 – ***Microglia morphology captured with cLSM and 2P-LSM. Microglia raw images obtained from cLSM (A) and 2P-LSM [in fixed tissue (B) and* in vivo *(C)] were used for segment branch tracing and data analysis. Each segment order is coded with different colors from red (first order branching) to green (fifth and higher branch order). For additional control, merge images were generated before data retrieval. Scale bar: 25 µm. cLSM: Confocal laser scanning microscopy; 2P-LSM: Two-photon laser scanning microscopy.***

License

This study was carried out at the University of Saarland in strict compliance with the recommendations of European and German guidelines for the welfare of experimental animals. Animal experiments were approved by the Saarland "Landesamt für Gesundheit und Verbraucherschutz" in Saarbrücken/Germany (Animal License No. 71/2010).

Results

Difference in image quality between laser scanning microscopy techniques

Although both acquisition technologies use lasers to excite EGFP and photomultiplier tubes for detection, we wanted, first, to evaluate the picture quality. The main problem was due to different pixel time and averaging in data acquisition. Therefore, we generated mean pixel intensity histograms (Figure 2A) and compared the mean intensity of pixels generating for all data sets (Figure 2B). The histogram revealed clear differences between cLSM and 2P-LPM (both *in vivo* and fixed tissues). cLSM used less grey tones than both 2P-LSM samples. The mean pixel intensity revealed differences, not only between cLSM and *in vivo* 2P-LSM, but also between *in vivo* and fixed tissue 2P-LSM (Figure 2B). We were not able to measure the power going into the sample but we did evaluate the average output laser power used for imaging. This showed that cLSM had approximately 300–350 mW, for our samples, while 2P-LSM used 650–750 mW for fixed tissue and 150 to 300 mW for *in vivo* imaging, depending on how deep the image was acquired. For this study, images were acquired at a depth between 100 and 200 µm.

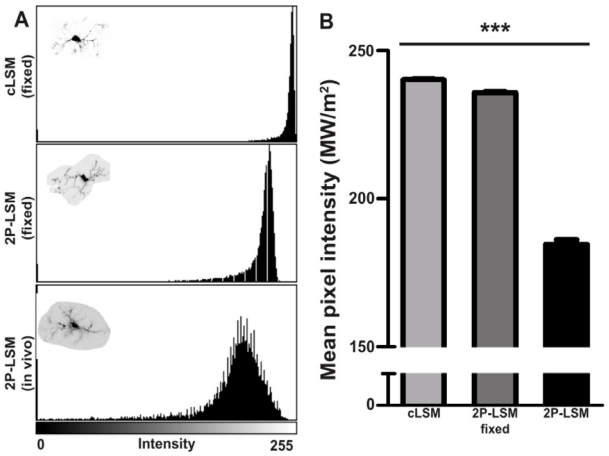

Figure 2 – ***Comparison between cLSM and 2P-LSM reveal different mean pixel intensities. When image qualities are compared between cLSM and 2P-LSM, the pixel histogram distribution shows a difference in grey pixel intensity between cLSM and 2P-LSM, already indicated in the original figures [inlets in (A)]. Comparison of mean pixel intensity (B) generated by cLSM and 2P-LSM (both for fixed tissue and* **in vivo***) shows significant higher mean pixel intensities in cLSM compared to 2P-LSM. cLSM: Confocal laser scanning microscopy; 2P-LSM: Two-photon laser scanning microscopy.***

Normal microglia morphology varies on the acquisition technique

To analyze global microglia morphology, branches were characterized by the average number of processes per cell and by the mean segment length. Using cLSM, a higher mean branch number could be determined than by using 2P-LSM (Figure 3A). Interestingly, 2P-LSM could not detect more branches *in vivo* compared to fixed tissue. Mean length of microglia segments also did not differ between the two methods ($p>0.05$) (Figure 3B).

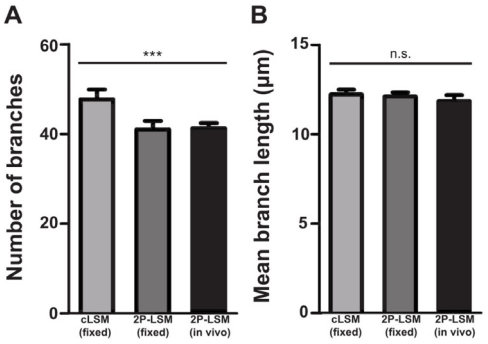

Figure 3 – ***More precise analysis of microglia morphology captured with cLSM and 2P-LSM reveals difference in branch numbers. There was a significant decrease in the number of detected branches when using 2P-LSM compared with cLSM (p<0.001) (A), however when analyzing the mean branch length, no difference could be detected (B). cLSM: Confocal laser scanning microscopy; 2P-LSM: Two-photon laser scanning microscopy; n.s.: Not significant.***

For a more precise evaluation of microglia morphology, the segments were classified into five different categories, according to their branch order (Figure 4, A–C). For each branch order, both mean length and average number were analyzed. No difference was found in the first four branch orders when number of branches determined with each method was compared. There was, however, a difference between the average discriminated number of branches in the fifth and higher order of ramification using cLSM compared to both *in vivo* and fixed 2P-LSM ($p<0.05$) (Figure 4D). This data suggests that the average increase in total number of branches found is due to better discrimination of fifth and higher order branch by cLSM, compared with 2P-LSM.

To exclude the possibility that 2P-LSM loses discrimination power in fine cellular morphology, mean length of each order segment was analyzed. No significant difference could be found between the average length of microglial segments ($p>0.05$) (Figure 4E).

Discussions

Microglia morphology is still extremely difficult to evaluate, even with more and more powerful computers and more sophisticated detection methods. Due to the complex and intricate microdomains of microglia, detailed, normal microglia analysis could be an important tool for studies that focus on small microglia changes, especially in borderline pathological conditions, as the aging brain [19, 35]. Here, we opted for this study for a semi-manual method that allowed a precise arbor tracking, as to eliminate small differences that could appear from the software algorithm itself.

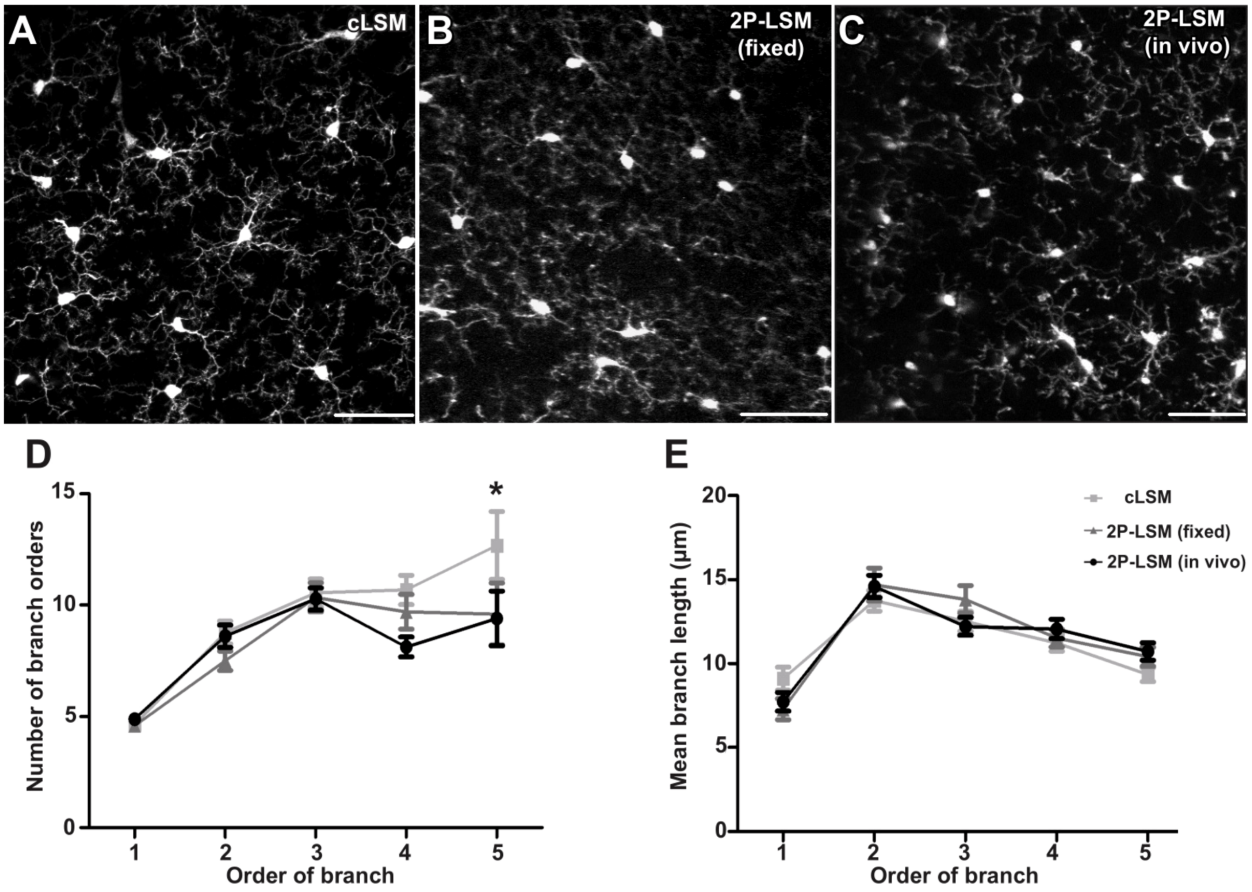

Figure 4 – ***Precise branch order analysis reveals difference in higher branch orders. Overview of analyzed microglial cells imaged with cLSM (A), fixed 2P-LSM (B) and* in vivo *2P-LSM (C) reveals difference in visual quality between the methods. Analysis of branch numbers sorted by order shows no difference between first and fourth order, while the fifth is changed significantly, with 2P-LSM less branches of the fifth order could be detected (D). No difference could be observed when mean branch length was analyzed (E). Scale bars indicate 50 µm. cLSM: Confocal laser scanning microscopy; 2P-LSM: Two-photon laser scanning microscopy.***

Technologies like cLSM, that helped researchers to collect detailed morphological information on specific cells types, are mostly able to generate still images of brain cells, which is not as different, from a physiological stand point than the classical wide field methods. Although, cLSM could be used both *in vitro* and *in vivo* experiments, due to how images are generated using this technique, it is not the standard for *in vivo* laser scanning microscopy. More and more peer reviewers will now ask authors to confirm their cLSM findings by 2P-LSM. This has determined us to compare morphological results obtain with these two methods. First, comparing the laser power and image quality we can see the one photon excitation used in cLSM needs more power than 2P-LSM. However, due to the pinhole method used, cLSM is able to generate better images, with a high signal to noise ratio. Interestingly, although this ratio improved in 2P-LSM if fixed tissue, the image quality was still visually inferior to cLSM. This is rather counterintuitive, as one will expect the same light scattering in slices, independent of the imaging method. However, this seems not to be the case. One explanation could be the use of averaging in cLSM compared with no averaging in 2P-LSM. Due to the averaging method used, the total scanning time per layer is higher in cLSM, than 2P-LSM, even if pixel time for the two methods is similar. Although it is technically possible to use averaging in 2P-LSM, such an approach is not used for *in vivo* applications, especially when investigating high dynamic cells like microglia. Because of this, we decided not to use averaging for fixed tissue 2P-LSM acquisition.

Initially, we thought that the lower number of branches detected by 2P-LSM is due to the perfusion method [24, 25]. We wanted to show that this was a consequence of the method for obtaining the sample and not of the imaging technique, therefore we decided to scan fix brain slices using the 2P-LSM. We were surprised to see that, even in fixed tissue samples, 2P-LSM can detect the same number of branches as *in vivo* imaging. This could be a matter of averaging, but the fact that all methods used were detecting the same mean branch length determined us to have a better look at which branches was 2P-LSM failing to detect. The better spatial resolution of cLSM was able to detect more fifth order branches compared with 2P-LSM (both *in vivo* and fixed tissue) with no difference in the average length of each branch order.

Conclusions

As more and more data is generated, there is an increasing tendency to amalgamate information without taking into consideration differences in the acquisition

methods. This can be helpful establishing validity and/or confirming new hypotheses. However, as we showed, even related technologies as cLSM and 2P-LSM do not overlap exactly. Although results from the two technologies can be discussed and even compared, the small differences between them should be taken into consideration when formulating a conclusion that is purely based on pure microscopic findings. This is especially applicable to microglia studies, where morphology is linked to its immune state. Furthermore, in our opinion, due to their highly dynamic nature, microglia should be carefully labeled as resting or active, taking also into consideration the imaging method used to obtain data.

Conflict of interests

The authors declare that they have no conflict of interests.

Author contribution

Smaranda Ioana Mitran and Emilia Burada have equally contributed to this paper.

Acknowledgments

We thank Anja Scheller and Laura Stopper, Department of Molecular Physiology, CIPMM (Center for Integrative Physiology and Molecular Medicine), University of Saarland, Germany, for allowing us to analyses some of their raw data. We are also grateful to Bogdan Cătălin for the support regarding the analyzed method used and comments on the manuscript. TAB was financed by the Romanian National Authority for Scientific Research and Innovation, CNCS–UEFISCDI, project number PN-III-P2-2.1-PED-2016-0803, within PNCDI III (Contract No. 143PED/2017).

References

[1] Mildner A, Schlevogt B, Kierdorf K, Böttcher C, Erny D, Kummer MP, Quinn M, Brück W, Bechmann I, Heneka MT, Priller J, Prinz M. Distinct and non-redundant roles of microglia and myeloid subsets in mouse models of Alzheimer's disease. J Neurosci, 2011, 31(31):11159–11171.

[2] Giaume C, Kirchhoff F, Matute C, Reichenbach A, Verkhratsky A. Glia: the fulcrum of brain diseases. Cell Death Differ, 2007, 14(7):1324–1335.

[3] Kettenmann H, Kirchhoff F, Verkhratsky A. Microglia: new roles for the synaptic stripper. Neuron, 2013, 77(1):10–18.

[4] Cătălin B, Cupido A, Iancău M, Albu CV, Kirchhoff F. Microglia: first responders in the central nervous system. Rom J Morphol Embryol, 2013, 54(3):467–472.

[5] Davalos D, Grutzendler J, Yang G, Kim JV, Zuo Y, Jung S, Littman DR, Dustin ML, Gan WB. ATP mediates rapid microglial response to local brain injury *in vivo*. Nat Neurosci, 2005, 8(6):752–758.

[6] Nimmerjahn A, Kirchhoff F, Helmchen F. Resting microglial cells are highly dynamic surveillants of brain parenchyma *in vivo*. Science, 2005, 308(5726):1314–1318.

[7] Walker FR, Beynon SB, Jones KA, Zhao Z, Kongsui R, Cairns M, Nilsson M. Dynamic structural remodelling of microglia in health and disease: a review of the models, the signals and the mechanisms. Brain Behav Immun, 2014, 37:1–14.

[8] Cătălin B, Alexandru D, Albu C, Iancău M. Microglia branching using a Sholl analysis method. Curr Health Sci J, 2013, 39(Suppl 4):1–5.

[9] Yamada J, Jinno S. Novel objective classification of reactive microglia following hypoglossal axotomy using hierarchical cluster analysis. J Comp Neurol, 2013, 521(5):1184–1201.

[10] Davis EJ, Foster TD, Thomas WE. Cellular forms and functions of brain microglia. Brain Res Bull, 1994, 34(1):73–78.

[11] Streit WJ, Walter SA, Pennell NA. Reactive microgliosis. Prog Neurobiol, 1999, 57(6):563–581.

[12] Stence N, Waite M, Dailey ME. Dynamics of microglial activation: a confocal time-lapse analysis in hippocampal slices. Glia, 2001, 33(3):256–266.

[13] Osiac E, Bălşeanu TA, Mogoantă L, Gheonea DI, Pirici I, Iancău M, Mitran SI, Albu CV, Cătălin B, Sfredel V. Optical coherence tomography investigation of ischemic stroke inside a rodent model. Rom J Morphol Embryol, 2014, 55(3):767–772.

[14] Osiac E, Bălşeanu TA, Cătălin B, Mogoantă L, Gheonea C, Dinescu SN, Albu CV, Cotoi BV, Tica OS, Sfredel V. Optical coherence tomography as a promising imaging tool for brain investigations. Rom J Morphol Embryol, 2014, 55(2 Suppl): 507–512.

[15] Streit WJ, Mrak RE, Griffin WS. Microglia and neuroinflammation: a pathological perspective. J Neuroinflammation, 2004, 1(1):14.

[16] Napoli I, Neumann H. Microglial clearance function in health and disease. Neuroscience, 2009, 158(3):1030–1038.

[17] Graeber MB. Changing face of microglia. Science, 2010, 330(6005):783–788.

[18] Cătălin B, Mitran S, Ciorbagiu M, Osiac E, Bălşeanu TA, Mogoantă L, Dinescu SN, Albu CV, Mirea CS, Vîlcea ID, Iancău M, Sfredel V. Microglial voltage-gated sodium channels modulate cellular response in Alzheimer's disease – a new perspective on an old problem. Rom J Morphol Embryol, 2015, 56(1):21–25.

[19] Popa-Wagner A, Carmichael ST, Kokaia Z, Kessler C, Walker LC. The response of the aged brain to stroke: too much, too soon? Curr Neurovasc Res, 2007, 4(3):216–227.

[20] Badan I, Buchhold B, Hamm A, Gratz M, Walker LC, Platt D, Kessler Ch, Popa-Wagner A. Accelerated glial reactivity to stroke in aged rats correlates with reduced functional recovery. J Cereb Blood Flow Metab, 2003, 23(7):845–854.

[21] Schafer DP, Lehrman EK, Kautzman AG, Koyama R, Mardinly AR, Yamasaki R, Ransohoff RM, Greenberg ME, Barres BA, Stevens B. Microglia sculpt postnatal neural circuits in an activity and complement-dependent manner. Neuron, 2012, 74(4):691–705.

[22] Wake H, Moorhouse AJ, Jinno S, Kohsaka S, Nabekura J. Resting microglia directly monitor the functional state of synapses *in vivo* and determine the fate of ischemic terminals. J Neurosci, 2009, 29(13):3974–3980.

[23] Tremblay MÈ, Lowery RL, Majewska AK. Microglial interactions with synapses are modulated by visual experience. PLoS Biol, 2010, 8(11):e1000527.

[24] Cătălin B, Stopper L, Bălşeanu TA, Scheller A. The *in situ* morphology of microglia is highly sensitive to the mode of tissue fixation. J Chem Neuroanat, 2017, 86:59–66.

[25] Stopper L, Bălşeanu TA, Cătălin B, Rogoveanu OC, Mogoantă L, Scheller A. Microglia morphology in the physiological and diseased brain – from fixed tissue to *in vivo* conditions. Rom J Morphol Embryol, 2018, 59(1):7–12.

[26] Shaw PJ. Comparison of widefield/deconvolution and confocal microscopy for three-dimensional imaging. In: Pawley J (ed). Handbook of biological confocal microscopy. Springer, New York, 2005, 453–467.

[27] Kurtz R. Bright solutions to get sharp images: confocal and two-photon fluorescence microscopy and the pros and cons of new multifocal approaches. In: Méndez-Vilas A, Díaz J (eds). Modern research and educational topics in microscopy. Vol. 1, Book Series "Microscopy", Formatex, Badajoz, 2007, 154–163.

[28] Masters B, So P. Confocal microscopy and multi-photon excitation microscopy of human skin *in vivo*. Opt Express, 2001, 8(1):2–10.

[29] Periasamy A, Skoglund P, Noakes C, Keller R. An evaluation of two-photon excitation *versus* confocal and digital deconvolution fluorescence microscopy imaging in *Xenopus* morphogenesis. Microsc Res Tech, 1999, 47(3):172–181.

[30] Jung S, Aliberti J, Graemmel P, Sunshine MJ, Kreutzberg GW, Sher A, Littman DR. Analysis of fractalkine receptor CX(3)CR1 function by targeted deletion and green fluorescent protein reporter gene insertion. Mol Cell Biol, 2000, 20(11):4106–4114.

[31] Cupido A, Catalin B, Steffens H, Kirchhoff F. Surgical procedures to study microglial motility in the brain and in the spinal cord by *in vivo* two-photon laser-scanning microscopy. In: Bakota L, Brandt R (eds). Laser scanning microscopy and

quantitative image analysis of neuronal tissue. Vol. 87, Book Series "Neuromethods", Humana Press, New York, 2014, 37–50.

[32] Pologruto TA, Sabatini BL, Svoboda K. ScanImage: flexible software for operating laser scanning microscopes. Biomed Eng Online, 2003, 2:13.

[33] Dibaj P, Nadrigny F, Steffens H, Scheller A, Hirrlinger J, Schomburg ED, Neusch C, Kirchhoff F. NO mediates microglial response to acute spinal cord injury under ATP control *in vivo*. Glia, 2010, 58(9):1133–1144.

[34] Meijering E, Jacob M, Sarria JC, Steiner P, Hirling H, Unser M. Design and validation of a tool for neurite tracing and analysis in fluorescence microscopy images. Cytometry A, 2004, 58(2): 167–176.

[35] Junker H, Suofu Y, Venz S, Sascau M, Herndon JG, Kessler C, Walther R, Popa-Wagner A. Proteomic identification of an upregulated isoform of annexin A3 in the rat brain following reversible cerebral ischemia. Glia, 2007, 55(16):1630–1637.

Corresponding authors

Tudor-Adrian Bălşeanu, Associate Professor, MD, PhD, Center of Clinical and Experimental Medicine, University of Medicine and Pharmacy of Craiova, 2 Petru Rareş Street, 200349 Craiova, Romania; Phone +40351–443 500 int. 2205, e-mail: adrian.balseanu@umfcv.ro

Cecil Sorin Mirea, Lecturer, MD, PhD, Department of Surgery, University of Medicine and Pharmacy of Craiova, 2 Petru Rareş Street, 200349 Craiova, Romania; Phone +40351–443 500, e-mail: mirea_cecil@yahoo.com

Received: November 10, 2017

Accepted: May 23, 2018